Letter

Evidence for valence-bond pairing in a one-dimensional two-orbital system

M. Mierzejewski [1], E. Dagotto [2,3] and J. Herbrych [1]

[1] Institute of Theoretical Physics, Faculty of Fundamental Problems of Technology, Wrocław University of Science and Technology, 50-370 Wrocław, Poland

[2] Department of Physics and Astronomy, University of Tennessee, Knoxville, Tennessee 37996, USA

[3] Materials Science and Technology Division, Oak Ridge National Laboratory, Oak Ridge, Tennessee 37831, USA

(Received 28 November 2024; revised 19 June 2025; accepted 24 June 2025; published 7 July 2025)

Valence bond (VB) states as the formation mechanism of Cooper pairs, eventually leading to high-temperature superconductivity, remain a controversial topic. Although various VB-like states find variational relevance in the description of specific spin models and quantum spin liquids, in the realm of many-body fermionic Hamiltonians, the evidence for such states as ground-state wave functions remains elusive, challenging the valence-bond pairing mechanism. Here, we present evidence of a VB ground state with pairing tendencies, particularly at finite doping. We achieved this for the generic two-orbital Hubbard model in low dimension, where the VB states can be associated with the presence of the topological order manifested by edge states.

DOI: 10.1103/qyqw-yy3j

Introduction. In 1987, just one year after the discovery of high-temperature superconductivity (high-T_c SC) in cuprates [1], Anderson proposed [2] his famous resonating valence bond (RVB) state as the ground-state wave function to describe the properties of such compounds. In essence, the RVB represents a quantum liquid of valence bonds, i.e., a collection of spin singlets, distributed over the lattice in a way that preserves its spatial symmetries. Note that the singlets are not necessarily nearest neighbors and can span over a few lattice sites, though their amplitude is expected to decay exponentially with distance. Such a state can, in principle, describe the Mott insulators' spin arrangement for the half electronic filing [3] and, more importantly, allow for mobile Cooper pairs under hole or electron doping (with each pair of holes or electrons "replacing" one of the singlets) [4,5].

Anderson's idea sparked enormous interest in the antiferromagnetic (AFM) Heisenberg models, which properly describe the main experimental findings of undoped cuprates [6,7] and parent compounds of some iron-based superconductors [8]. However, the RVB and even more generic valence bond solids (VBSs, which break some of the lattice symmetry) are rare as the ground-state wave functions of the many-body systems. For the spin models, notable examples of such states exist.

(i) It has been established that quantum spin liquids [9] realized in geometrically frustrated magnets [10,11] can be described by the RVB wave function.

(ii) The ground states of the one-dimensional (1D) $S = 1/2$ Heisenberg model with nearest- and next-nearest-neighbor interaction (the so-called Majumdar-Ghosh model) [12,13] or the two-dimensional (2D) Shastry-Sutherland model [14] are exact VBS states.

(iii) Finally, it has been shown [15,16] that the $S = 1$ Heisenberg chain with biquadratic interactions can be thought of as a collection of coupled $S = 1/2$-like singlets [Fig. 1(a)].

The latter is encapsulated in the Affleck-Kennedy-Lieb-Tasaki state (AKLT state), which hosts the famous topological Haldane edge states. It is important to note that the AKLT state is a perfect VBS. At the same time, the plain $S = 1$ Heisenberg model in 1D resembles a gapped RVB state with exponentially decaying correlations [17].

In the context of fermionic Hamiltonians, evidence of a valence bond (VB)-like state as the ground state of the many-body system is still lacking. Although such states are anticipated to capture many properties of quantum paramagnets, the challenge is demonstrating that the ground state has a form of VB liquid. Here, we report the evidence that the ground state of the generic two-orbital Hubbard model in low-dimension realizes a VB-like state. The latter maintains the topological properties of the AKLT state and, in addition, becomes superconducting at finite doping. Namely, we show that the topology and pairing are intertwined in the doped fermionic Haldane chain. Although limited to 1D considerations, our density-matrix renormalization group (DMRG) calculations reveal most of the properties expected of the high-T_c phase diagram, i.e., (i) a large region of finite binding energy in the interaction-doping phase diagram, (ii) long-range of pair-pair correlations, and (iii) pair density wave (PDW). We also show that (iv) all of these phenomena are induced by the VB ground state akin to the AKLT state of $S = 1$ Heisenberg chains. Since the latter exhibits topological properties, the presence of VB-type states can be easily identified via the presence of the topological order.

Orbital-RVB. Our investigation is based on the two-orbital ($\gamma = 0$ and 1) Hubbard-Kanamori model on the 1D lattice:

$$
\begin{aligned}
H = t \sum_{\gamma\gamma'\ell\sigma} (c^{\dagger}_{\gamma\ell\sigma} c_{\gamma'\ell+1\sigma} + \text{H.c.}) \\
+ U \sum_{\gamma\ell} n_{\gamma\ell\uparrow} n_{\gamma\ell\downarrow} + U' \sum_{\ell} n_{0\ell} n_{1\ell} \\
- 2J_{\text{H}} \sum_{\ell} \mathbf{S}_{0\ell} \cdot \mathbf{S}_{1\ell} + J_{\text{H}} \sum_{\ell} (P^{\dagger}_{0\ell} P_{1\ell} + \text{H.c.}),
\end{aligned}
\quad (1)
$$

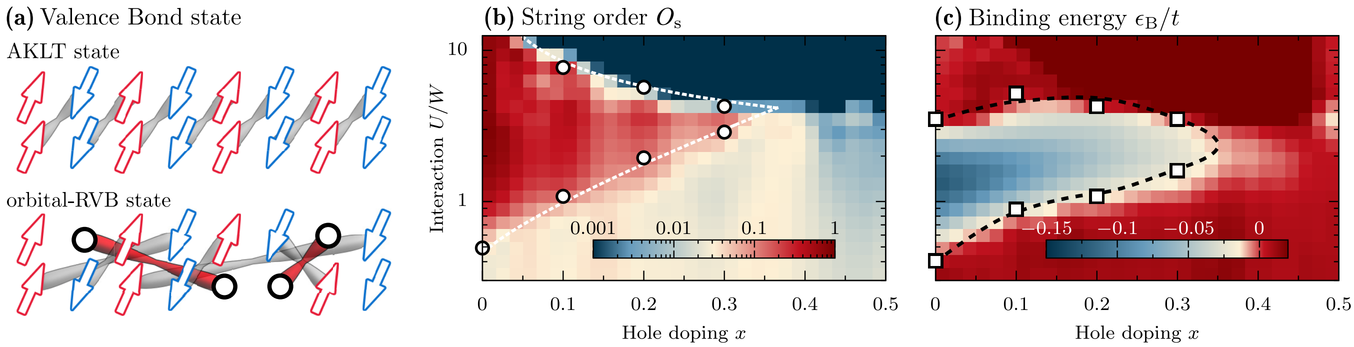

FIG. 1. (a) Sketch of the AKLT state (top) and the orbital-RVB state of the doped one-dimensional two-orbital Hubbard model (lower). Paired holes are presented as circles. (b) Interaction U–doping x phase diagram of the string order parameter O_s evaluated in the bulk (at distance $\ell = L/2$) of the $L = 60$ sites system. The points depict values at which extrapolated to $L \to \infty$ spin gap Δ_S opens or closes. (c) Phase diagram for binding energy $\epsilon_B = E_{gs}(N) - 2E_{gs}(N-1) + E_{gs}(N-2)$, where $E_{gs}(N)$ is the energy of the fermionic system with N electrons ($L = 60$). Points depict values at which the extrapolated to $L \to \infty$ binding energy crosses the zero value. Lines are a guide to the eye.

with $P^\dagger_{\gamma\ell} = c^\dagger_{\gamma\ell\uparrow}c^\dagger_{\gamma\ell\downarrow}$. In the following, we consider its most generic version, with band degeneracy. The first term describes the system's kinetic energy (with the kinetic energy span given by $W = 4t$). The second term describes intraorbital (U) and interorbital (U') on-site electron repulsion. The last term originates in multiorbital physics: J_H accounts for the ferromagnetic Hund coupling between spins $\mathbf{S}_{\gamma\ell}$ at different orbitals, maximizing the total on-site spin. The above model preserves SU(2) symmetry (provided that $U' = U - 5/2J_H$ [18]), and we consider $J_H/U = 1/4$ in the $S^z_{tot} = 0$ magnetization sector for various hole doping levels $x = 1 - \overline{n}$, where $\overline{n} = N/2L$ is electron density (with N being the number of electrons in an L-site system). The quasi-1D (ladders) and 2D versions of the above model are extensively used in the context of various correlated superconductors like iron pnictides, chalcogenides, ruthenates, iridates, and heavy-fermion materials. In the following, we present results obtained with the help of the DMRG method on the open-boundary system (see Supplemental Material [19] and Refs. [20–22] therein for details).

At half-filling $x = 0$ and in the limit of large interaction strength $U \gg W$, i.e., in the region where double occupancies are not present and the average on-site magnetic moments are well developed $\mathbf{S}^2 = S(S+1) \simeq 2$, the low-energy physics of the two-orbital Hubbard model can be described by the $S = 1$ AFM Heisenberg Hamiltonian [23]. The ground state of the latter can be pictorially expressed [Fig. 1(a)] by on-site triplets of $S = 1/2$-like objects, i.e.,

$$|1_i\rangle = |\uparrow_{0i}\uparrow_{1i}\rangle, \quad |-1_i\rangle = |\downarrow_{0i}\downarrow_{1i}\rangle,$$
$$|0_i\rangle = \frac{1}{\sqrt{2}}(|\uparrow_{0i}\downarrow_{1i}\rangle + |\downarrow_{0i}\uparrow_{1i}\rangle),$$

which are coupled in a valence bond way between sites, $(1/\sqrt{2})(|\uparrow_{0i}\downarrow_{1i+1}\rangle - |\downarrow_{0i}\uparrow_{1i+1}\rangle)$. Here $|1,0,-1\rangle$ represent $S = 1$ states at site i, while $|\sigma_{\gamma i}\sigma_{\gamma' j}\rangle$ with $\sigma_i = \uparrow,\downarrow$ can be thought of as a spin configuration of two electrons at different orbitals γ and γ' in the context of the two-orbital Hubbard model. The above VBS (AKLT state) is not an exact ground state of the isotropic $S = 1$ AFM model. Still, it can be adiabatically connected to it without closing the spin gap and preserving its unique properties, i.e., the presence of the topologically protected Haldane edge states (unpaired by valence bonds' $S = 1/2$ states at the boundary of the open system). It has recently been shown [23] that such a description of the two-orbital Hubbard model in 1D is valid even for a relatively small value of interaction, $U \simeq W/2$, in the region where magnetic moments are not fully developed $\mathbf{S}^2 \ll 2$ and charge fluctuations are still present. Such behavior can be monitored with the help of the string order correlation function:

$$O_s(\ell) = -\langle \mathrm{gs}|S^z_m \exp\left(i\pi \sum_{n=m+1}^{m+\ell-1} S^z_n\right) S^z_{m+\ell}|\mathrm{gs}\rangle, \tag{2}$$

with $|\mathrm{gs}\rangle$ being the ground-state wave function and $S^z_m = S^z_{0m} + S^z_{1m}$ being the total spin at site m, which serves as the order parameter of the AKLT state in the $\ell \to \infty$ limit (i.e., breaking of the discrete $Z_2 \times Z_2$ hidden symmetry).

Introduction of the holes into the AKLT state is a nontrivial task. In principle, two scenarios are possible in the atomic limit: the formation of "rigid" on-site holes $|h_{0i}h_{1i}\rangle$ in the AFM $S = 1$ background or the pair of holes transforming two of the $S = 1$ on-site triplets into two $S = 1/2$ objects, e.g.,

$$|\uparrow_{0i}\downarrow_{1i}\rangle - |\downarrow_{0i}\uparrow_{1i}\rangle \quad \to \quad |\uparrow_{0i}h_{1i}\rangle - |h_{0i}\uparrow_{1i}\rangle.$$

In the atomic limit $t = 0$, the former scenario is favored by the Hund exchange J_H since it is maximizing the average magnetic moments. On the other hand, the latter case—with one hole per site—is preferred by the interorbital repulsion U' term in the Hamiltonian. To resolve this state in the many-body system $t \neq 0$, we monitor the behavior of the ground state with doping x and interaction U by evaluating the string order parameter $O_s(\ell)$. Detailed distance dependence is presented in Fig. 2(a), while Fig. 1(b) depicts the phase diagram obtained from the bulk value of $O_s(L/2)$ (see also Supplemental Material [19] for additional results). For dopings $x \lesssim 0.35$, one can observe a region where the string order parameter is finite, excluding two holes at the same site (but different orbitals $|h_{i0}h_{i1}\rangle$), which would break the AFM chain into two parts. More importantly, our results are consistent with a one hole per site scenario, i.e., with (two) holes replacing one of

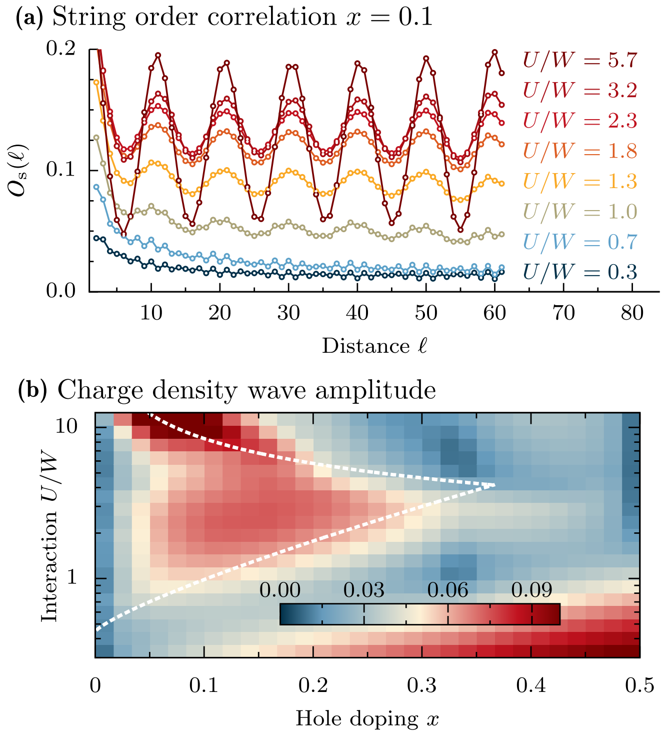

FIG. 2. (a) Distance dependence of string order correlation function $O_s(\ell)$ for various values of interaction strength U/W and $x = 0.1$ hole-doped system ($L = 80$ data). (b) Amplitude of the charge density oscillations ($L = 60$). Lines represent the same guide to the eye as in Fig. 1.

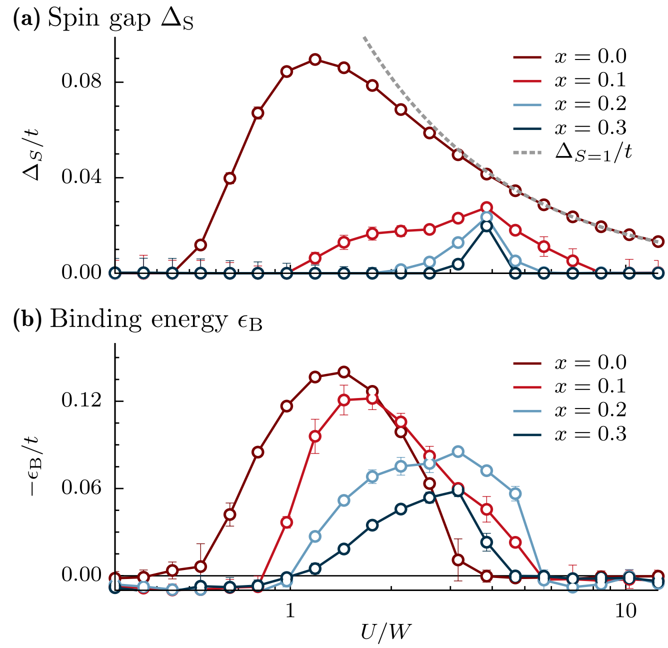

FIG. 3. Extrapolated to $L \to \infty$ (a) spin gap $\Delta_S = E_{gs}(S^z_{tot} = 2) - E_{gs}(S^z_{tot} = 0)$ and (b) binding energy $-\epsilon_B$. The dashed line in panel (a) indicates the Haldane gap $\Delta_{S=1} = 0.41J$ with $J = 2t^2/(U + J_H)$.

the valence bonds. For a few holes away from half-filling, $x = 0$, such a state was coined the orbital-RVB [24–26]. Here, we extend this definition to rather large doping levels, $x \simeq 0.35$, and show that its properties are consistent with the valence-bond pairing mechanism.

For $x = 0$ (half-filling), one can observe [Fig. 1(b)] a finite string-order parameter for all $U/W \gtrsim 0.5$ (with the $U \to \infty$ limit given by the $S = 1$ Heisenberg model), while for $x \neq 0$ this is true only in a finite region of interaction strength U. One can understand the lower (at small U) topological phase transition (from trivial paramagnetic to topological orbital-RVB state) as an effect of interaction U strengthening the magnetic moments $\mathbf{S}$ and decreasing the charge fluctuations. On the other hand, the upper (at large U) transition is associated with the change in the spin-spin correlations from AFM (incommensurate at finite x) to ferromagnetic (FM) ordering due to double-exchange-like physics in the large Hund limit for $x \neq 0$ [27,28]. In the Supplemental Material [19] (see also references [29–37] therein), we also present the analysis of the correlations between the system's edges, confirming the presence of topologically protected edge states, and the spin-spin magnetic structure factor analysis confirming the AFM to FM transition at large U.

Since the orbital-RVB state shares its topological properties with the "standard" AKLT state, one expects that finite string order $O_s \neq 0$ is accompanied by the presence of the reminiscence of the Haldane gap ($\Delta_{S=1} \simeq 0.41J$ for the $x = 0$ AKLT state, with spin exchange $J = 2t^2/(U + J_H)$ [23]). In Fig. 3(a), we present the interaction U dependence of the (extrapolated to thermodynamic limit [19]) spin gap Δ_S. Indeed, our results indicate that Δ_S remains open in the same region where the string order is finite, also for nonzero doping $x \neq 0$ [see points presented in Fig. 1(b), which depict opening and closing of the spin gap].

Finally, the spatial dependence of the string order parameter $O_s(\ell)$ indicates the presence of pronounced oscillations for $x \neq 0$. We associate them with the presence of Friedel oscillations in the charge sector (due to the open-boundary system), visible also in the site-resolved electron density $n_\ell = n_{0\ell} + n_{1\ell}$ (see the Supplemental Material [19]). In Fig. 2(b), we present the spatial standard deviation of the density $\sigma_n = \sqrt{(1/L)\sum_\ell n_\ell^2 - \overline{n}^2}$, related to the amplitude A of the cosine wave, $\sigma_n \simeq A/\sqrt{2}$. In the topologically trivial region, $U \lesssim W$ and $x \gtrsim 0.2$, we find the "standard" $2k_F = \pi\overline{n} = \pi(1 - x) \propto \pi x$ charge-density-wave oscillations of a weakly interacting system. Interestingly, in the region where we find finite $O_s \neq 0$ ($U \sim 2W$, $x \lesssim 0.35$), our results indicate that the charge oscillates with the $2\pi x$ wave vector. The latter is consistent with a PDW with $4k_F$ oscillations [38–40] (leading to two doped holes per one minimum in oscillation). This indicated that the PDW accompanies the doped orbital-RVB and is most pronounced at doping $x \simeq 0.15$.

Binding energy. Our results show that the orbital-RVB state remains robust even for large doping $x \simeq 0.3$ at $U \simeq 4W$. In Fig. 1(c), we contrast this behavior with the binding energy ϵ_B, where a negative value signals the presence of bound pairs of holes (or electrons for $x < 0$, due to the particle-hole symmetry of the considered model). The significant overlap in the interaction-doping phase diagram between the finite string order, $O_s \neq 0$, and the negative binding energy, $\epsilon_B < 0$, indicates that the VB structures of the ground state and bounded pairs coexist. Consequently, the latter are correlated

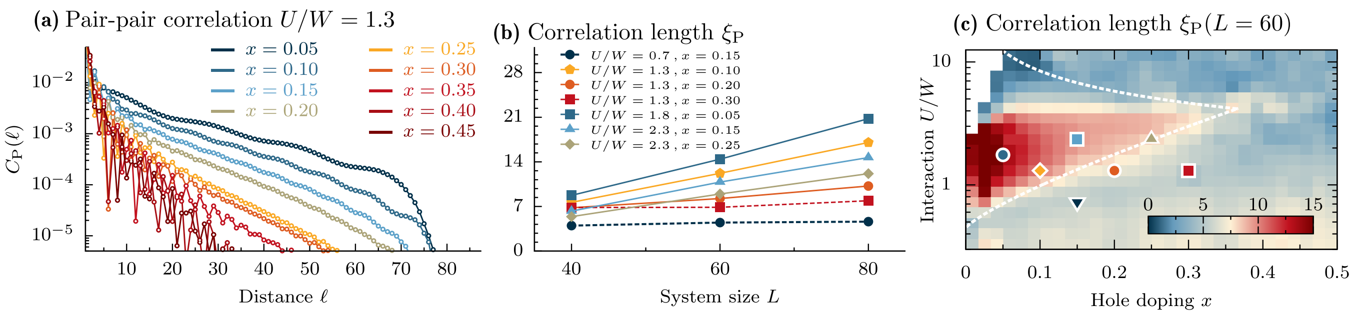

FIG. 4. (a) Doping x dependence of the pair-pair correlation function $C_P(\ell)$ for $U/W = 1.3$ ($L = 80$ data). (b) Finite-size scaling ($L = 40$, 60, and 80) of the pair-pair correlation length ξ_P obtained from $C_P(\ell) \propto \exp(-\ell/\xi_P)$ fits (see the Supplemental Material for more data [19]). (c) Phase diagram of the correlation length ξ_P obtained from the fits to the $L = 60$ sites system. Points depict parameters presented in panel (b). Lines represent the same lines that represent guides to the eye as in Fig. 1.

due to the former [see Fig. 1(a)]. The above behavior is in accord with the scenario envisioned by Anderson's proposal: upon doping, the system minimizes its energy by breaking a minimal amount of coupled singlets (valence bonds) [41]. Interestingly, the VB-induced pairing (as measured by negative binding energy) is found for the electron-electron interaction strengths U, which are "just below" the large interaction expansion, i.e., below the $J(U) \propto 1/U$ energy scale, which gives the proper description of the spin excitations.

It is important to note that the presence of the bounded pairs does not necessarily imply superconducting tendencies. The latter requires nonvanishing long-range correlations in the thermodynamic limit $L \to \infty$. One can monitor this with the Cooper pair susceptibility:

$$C_P(\ell) = \frac{1}{L-\ell} \sum_{i,\gamma\neq\gamma'} \langle \Delta^\dagger_{i\gamma\gamma'} \Delta_{i+\ell\gamma\gamma'} \rangle, \tag{3}$$

where $\Delta^\dagger_{i\gamma\gamma'}$ represent singlet pairs between nearest-neighbor sites at different orbitals, $\Delta^\dagger_{i\gamma\gamma'} = c^\dagger_{\gamma i\uparrow} c^\dagger_{\gamma' i+1\downarrow} - c^\dagger_{\gamma i\downarrow} c^\dagger_{\gamma' i+1\uparrow}$. Such a pairing is consistent with doping of the orbital-RVB state described above and with earlier numerical investigations [24]. Our results indicate two distinct behaviors (see Figs. 4(a) and 4(b) and the Supplemental Material [19]). For the trivial (non-VB) state (e.g., $x \gtrsim 0.25$ for $U = 1.3$), we observe fast exponential decay of the pair-pair correlation $C_P(\ell) \propto \exp(-\ell/\xi_P)$, with size-independent correlation length ξ_P [see Fig. 4(b)]. On the other hand, for the orbital-RVB states we find that the correlation length increases with system size, $\xi_P(L) \propto L^\alpha$, with $\alpha \simeq 1$. The analysis of the ξ_P value for a finite-size system [Fig. 4(c)] confirms that the correlation length in this region becomes large: $\xi_P(L = 60) \sim 20$. This implies that, even in the thermodynamic limit $L \to \infty$, the pairs in our VB state are correlated at distances of the order of the system size, again confirming Anderson's RVB pairing scenario.

Conclusions. Since our results are obtained on the one-dimensional two-orbital model with total $S = 1$ magnetic moments in the $U \gg W$ limit, the relevance of our results to cuprates is unknown (fundamentally considered as a single-orbital 2D system with $S = 1/2$). However, it is well established that the multiorbital nature of the Fermi surface plays a crucial role in the properties of iron-based superconductors. Consequently, the studied model is relevant for the latter. Consider the flagship iron-based superconductor Fe(Se,Te) [42,43]. The magnetism of this compound is believed [8,11,44] to be described by the frustrated J_1-J_2 $S = 1$ Heisenberg model in two dimensions. Interestingly, for the relevant $J_2/J_1 \sim 0.5$ values, the system ground state can be described [11,45,46] by spontaneously forming $S = 1$ AKLT-like chains. Furthermore, it is known [47] that odd-integer spin chains have topologically protected AKLT states. The latter can also be realized as frustrated multi-odd-leg $S = 1$ tubes [48]. In essence, with caveats that our minimal model does not consider, e.g., the nematic phase transition present upon doping, our results are "just" doping of such systems.

Our findings reveal an astonishing robustness of the Haldane physics of the $S = 1$ AFM chain upon hole doping (topologically nontrivial orbital-RVB state) and its importance for the pairing correlations even at significantly large doping levels ($x \simeq 0.35$). This is unexpected since such a phase is fragile for pure spin models [49,50]. Furthermore, our results encapsulate the main features expected in the superconductor's phase diagram at zero temperature: doping the quantum paramagnetic system leads to a finite region in which pair-pair correlations are present. This is especially appealing for $U \sim 4W$ ($U \sim 16t$), for which we see the above behavior for $0.1 \lesssim x \lesssim 0.3$. Furthermore, for $U \sim 2W$ and $0.2 < x < 0.35$, the pair-pair correlation decays relatively fast, although the binding energy is negative, $\epsilon_B < 0$. One can associate this with zero spin-gap Δ_S and preformed pairs in the vicinity of a trivial-topological transition (which becomes coherent at larger U, when $\Delta_S \neq 0$, i.e., in the topologically nontrivial region). However, our finite-size data cannot exclude a small but finite Δ_S already in this region. Finally, it is worth noting that the orbital-RVB state has a topological origin and is protected from perturbations that do not close the spin gap. Consequently, the specific values of the Hamiltonian parameters like the Hund exchange J_H or details of the kinetic energy and hybridization between orbitals will not change the overall properties of the system, as was previously shown for half-filling $x = 0$ [23].

Acknowledgments. J.H. acknowledges grant support from the National Science Centre (NCN), Poland, via Sonata BIS Project No. 2023/50/E/ST3/00033. The U.S. Department of Energy, Office of Science, Basic Energy Sciences, Materials Sciences and Engineering Division, supported E.D. Part of the calculations have been carried out using resources provided by the Wroclaw Centre for Networking and Supercomputing [51].

Data availability. The data that support the findings of this article are openly available [52].

[1] J. G. Bednorz and K. A. Müller, Possible high T_c superconductivity in the Ba-La-Cu-O system, Z. Phys. B **64**, 189 (1986).

[2] P. W. Anderson, The resonating valence bond state in La_2CuO_4 and superconductivity, Science **235**, 1196 (1987).

[3] S. Liang, B. Doucot, and P. W. Anderson, Some new variational resonating-valence-bond-type wave functions for the spin-1/2 antiferromagnetic Heisenberg model on a square lattice, Phys. Rev. Lett. **61**, 365 (1988).

[4] G. Baskaran, Z. Zou, and P. W. Anderson, The resonating valence bond state and high-Tc superconductivity—A mean field theory, Solid State Commun. **63**, 973 (1987).

[5] P. W. Anderson, G. Baskaran, Z. Zou, and T. Hsu, Resonating–valence-bond theory of phase transitions and superconductivity in La_2CuO_4-based compounds, Phys. Rev. Lett. **58**, 2790 (1987).

[6] H. Kageyama, K. Yoshimura, R. Stern, N. V. Mushnikov, K. Onizuka, M. Kato, K. Kosuge, C. P. Slichter, T. Goto, and Y. Ueda, Exact dimer ground state and quantized magnetization plateaus in the two-dimensional spin system $SrCu_2(BO_3)_2$, Phys. Rev. Lett. **82**, 3168 (1999).

[7] B. Dalla Piazza, M. Mourigal, N. B. Christensen, G. J. Nilsen, P. Tregenna-Piggott, T. G. Perring, M. Enderle, D. F. McMorrow, D. A. Ivanov, and H. M. Rønnow, Fractional excitations in the square-lattice quantum antiferromagnet, Nat. Phys. **11**, 62 (2015).

[8] J. K. Glasbrenner, I. I. Mazin, H. O. Jeschke, P. J. Hirschfeld, R. M. Fernandes, and R. Valenti, Effect of magnetic frustration on nematicity and superconductivity in iron chalcogenides, Nat. Phys. **11**, 953 (2015).

[9] L. Savary and L. Balents, Quantum spin liquids: A review, Rep. Prog. Phys. **80**, 016502 (2017).

[10] L. Balents, Spin liquids in frustrated magnets, Science **464**, 199 (2010).

[11] F. Wang, S. A. Kivelson, and D.-H. Lee, Nematicity and quantum paramagnetism in FeSe, Nat. Phys. **11**, 959 (2015).

[12] C. K. Majumdar and D. K. Ghosh, On next-nearest-neighbor interaction in linear chain. I, J. Math. Phys. **10**, 1388 (1969).

[13] C. K. Majumdar and D. K. Ghosh, On next-nearest-neighbor interaction in linear chain. II, J. Math. Phys. **10**, 1399 (1969).

[14] B. S. Shastry and B. Sutherland, Exact ground state of a quantum mechanical antiferromagnet, Physica B+C (Amsterdam) **108**, 1069 (1981).

[15] I. Affleck, T. Kennedy, E. H. Lieb, and H. Tasaki, Rigorous results on valence-bond ground states in antiferromagnets, Phys. Rev. Lett. **59**, 799 (1987).

[16] I. Affleck, T. Kennedy, E. H. Lieb, and H. Tasaki, Valence bond ground states in isotropic quantum antiferromagnets, Commun. Math. Phys. **115**, 477 (1988).

[17] I. Affleck, Quantum spin chains and the Haldane gap, J. Phys.: Condens. Matter **1**, 3047 (1989).

[18] A. Georges, L. de' Medici, and J. Mravlje, Strong correlations from Hund's coupling, Annu. Rev. Condens. Matter Phys. **4**, 137 (2013).

[19] See Supplemental Material at http://link.aps.org/supplemental/10.1103/qyqw-yy3j for (i) details of the DMRG method, (ii) additional data for string order and pair-pair correlation function, (iii) results for the static structure factor, and (iv) charge density oscillation analysis.

[20] S. R. White, Density matrix formulation for quantum renormalization groups, Phys. Rev. Lett. **69**, 2863 (1992).

[21] U. Schollwöck, The density-matrix renormalization group, Rev. Mod. Phys. **77**, 259 (2005).

[22] S. R. White, Density matrix renormalization group algorithms with a single center site, Phys. Rev. B **72**, 180403(R) (2005).

[23] A. Jażdżewska, M. Mierzejewski, M. Środa, A. Nocera, G. Alvarez, E. Dagotto, and J. Herbrych, Transition to the Haldane phase driven by electron-electron correlations, Nat. Commun. **14**, 8524 (2023).

[24] N. D. Patel, A. Nocera, G. Alvarez, A. Moreo, and E. Dagotto, Pairing tendencies in a two-orbital Hubbard model in one dimension, Phys. Rev. B **96**, 024520 (2017).

[25] N. Patel, N. Kaushal, A. Nocera, G. Alvarez, and E. Dagotto, Emergence of superconductivity in doped multiorbital Hubbard chains, npj Quantum Mater. **5**, 27 (2019).

[26] P. Laurell, J. Herbrych, G. Alvarez, and E. Dagotto, Luther-emery liquid and dominant singlet superconductivity in the hole-doped Haldane spin-1 chain, Phys. Rev. B **110**, 064515 (2024).

[27] T. Momoi and K. Kubo, Ferromagnetism in the Hubbard model with orbital degeneracy in infinite dimensions, Phys. Rev. B **58**, R567(R) (1998).

[28] K. Held and D. Vollhardt, Electronic correlations in manganites, Phys. Rev. Lett. **84**, 5168 (2000).

[29] C. Zener, Interaction between the d shells in the transition metals, Phys. Rev. **81**, 440 (1951).

[30] C. Zener, Interaction between the d-shells in the transition metals. II. Ferromagnetic compounds of manganese with perovskite structure, Phys. Rev. **82**, 403 (1951).

[31] F. F. Assaad and D. Würtz, Charge and spin structures in the one-dimensional t-J model, Phys. Rev. B **44**, 2681 (1991).

[32] M. Troyer, H. Tsunetsugu, T. M. Rice, J. Riera, and E. Dagotto, Spin gap and superconductivity in the one-dimensional t-J model with Coulomb repulsion, Phys. Rev. B **48**, 4002 (1993).

[33] H. Q. Lin, E. Gagliano, and D. K. Campbell, Phase separation in the 1-D extended Hubbard model, Phys. C: (Amsterdam, Neth.) **282-287**, 1875 (1997).

[34] J. Riera, K. Hallberg, and E. Dagotto, Phase diagram of electronic models for transition metal oxides in one dimension, Phys. Rev. Lett. **79**, 713 (1997).

[35] K. Haule and G. G Kotliar, Coherence–incoherence crossover in the normal state of iron oxypnictides and importance of Hund's rule coupling, New J. Phys. **11**, 025021 (2009).

[36] Q. Luo, G. Martins, D.-X. Yao, M. Daghofer, R. Yu, A. Moreo, and E. Dagotto, Neutron and ARPES constraints on the

couplings of the multiorbital Hubbard model for the iron pnictides, Phys. Rev. B **82**, 104508 (2010).

[37] J. Ferber, K. Foyevtsova, R. Valentí, and H. O. Jeschke, LDA + DMFT study of the effects of correlation in LiFeAs, Phys. Rev. B **85**, 094505 (2012).

[38] E. Berg, E. Fradkin, and S. A. Kivelson, Pair-density-wave correlations in the Kondo-Heisenberg model, Phys. Rev. Lett. **105**, 146403 (2010).

[39] Y.-H. Zhang and A. Vishwanath, Pair-density-wave superconductor from doping Haldane chain and rung-singlet ladder, Phys. Rev. B **106**, 045103 (2022).

[40] Y. Liu, T. Wei, G. He, Z. Zhang, Y. Wang, and J. Wang, Pair density wave state in a monolayer high-T_c iron-based superconductor, Nature (London) **618**, 934 (2023).

[41] E. Dagotto, J. Riera, and D. Scalapino, Superconductivity in ladders and coupled planes, Phys. Rev. B **45**, 5744 (1992).

[42] Q. Wang, Y. Shen, B. Pan, Y. Hao, M. Ma, F. Zhou, P. Steffens, K. Schmalzl, T. R. Forrest, M. Abdel-Hafiez, X. Chen, D. A. Chareev, A. N. Vasiliev, P. Bourges, Y. Sidis, H. Cao, and J. Zhao, Strong interplay between stripe spin fluctuations, nematicity and superconductivity in FeSe, Nat. Matter. **15**, 159 (2016).

[43] A. Kreisel, P. J. Hirschfeld, and B. M. Andersen, On the remarkable superconductivity of FeSe and its close cousins, Symmetry **12**, 1402 (2020).

[44] A. L. Wysocki, K. D. Belashchenko, and V. P. Antropov, Consistent model of magnetism in ferropnictides, Nat. Phys. **7**, 485 (2011).

[45] M. D. Watson, T. K. Kim, L. C. Rhodes, M. Eschrig, M. Hoesch, A. A. Haghighirad, and A. I. Coldea, Evidence for unidirectional nematic bond ordering in FeSe, Phys. Rev. B **94**, 201107(R) (2016).

[46] I. Niesen and P. Corboz, Emergent Haldane phase in the $S = 1$ bilinear-biquadratic Heisenberg model on the square lattice, Phys. Rev. B **95**, 180404(R) (2017).

[47] F. Pollmann, E. Berg, A. M. Turner, and M. Oshikawa, Symmetry protection of topological phases in one-dimensional quantum spin systems, Phys. Rev. B **85**, 075125 (2012).

[48] D. Charrier, S. Capponi, M. Oshikawa, and P. Pujol, Quantum phase transitions in three-leg spin tubes, Phys. Rev. B **82**, 075108 (2010).

[49] F. Anfuso and A. Rosch, Fragility of string orders, Phys. Rev. B **76**, 085124 (2007).

[50] S. Moudgalya and F. Pollmann, Fragility of symmetry-protected topological order on a Hubbard ladder, Phys. Rev. B **91**, 155128 (2015).

[51] http://wcss.pl.

[52] All data discussed in this paper are available at https://github.com/jacekherbrych/DataRepository.